THE ARCHIVE OF MECHANICAL ENGINEERING

Vol. LI 2004 Number 4

Key words: *electrochemical machining, ECM, electrolyte flow, computer simulation, vibrating electrode*

*LUCJAN DĄBROWSKI**), *TOMASZ PACZKOWSKI***)

2D COMPUTER SIMULATION OF PHENOMENA OCCURRING IN THE INTER-ELECTRODE GAP DURING ELECTROCHEMICAL MACHINING WITH VIBRATING ELECTRODE

In the paper, the authors present a mathematical and numerical model of two-dimensional electrolyte flow in an interelectrode gap. Computer software for flow simulation with the possibility of visualization of distribution of physical conditions during process has been elaborated. The proposed mathematical model of electrolyte flow was verified experimentally by comparing real profiles of machined surface with profiles obtained in computer simulation. For this purpose there was examined a case of machining with a vibrating electrode and without vibrations.

1. Introduction

Electrochemical machining with vibratory tool-electrode (TE) is today one of the basic operations of electrochemical technology for machine parts and devices. In the constant process, the TE most often performs translatory motion in the direction of the surface which is machined. Electrolyte is supplied with high velocity to the interelectrode gap (IEG) causing removal of machining products from the interelectrode gap. These are mainly hydrogen molecules and ions of dissolved metal. Thus, in such conditions we have a multiphase, three-dimensional flow [1]. Hydrodynamic parameters of the flow and the medium properties determine the processes of mass, momentum and energy transfer in the IEG. Correctly selected, they prevent from arising cavitation zones, critical flow, circulation and excessive temperature rise of

*) *Warsaw University of Technology, Institute of Production Engineering, Poland; E-mail: ld@meil.pw.edu.pl*

**) *University of Technology and Agriculture in Bydgoszcz, Faculty of Mechanical Engineering, Poland; E-mail: tompacz@atr.bydgoszcz.pl*

the electrolyte and volumetric concentration of the gas phase. The mentioned processes have significant impact on electrochemical dissolution velocity and applicability properties of the machined surface [2].

For the purpose of accuracy and stability of the ECM processing improvement, the TE vibrations is used. Introduction of TE vibrations causes that interelectrode gap thickness changes from S_{min} to S_{max} (Fig. 1) during the machining process. Minimal thickness S_{min} makes it possible to increase the machining accuracy, i.e. TE shape representation, and to obtain high current densities. When gap thickness is S_{max}, the current density decreases, and good electrolyte exchange conditions arise. The machining process reliability increases as well, because it is easier to avoid failure states occurrence.

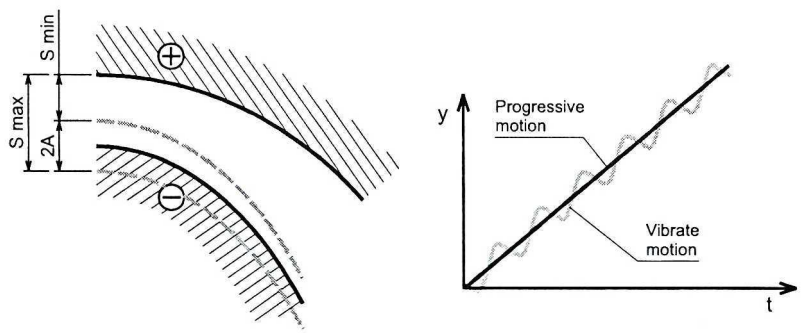

Fig. 1. Electrode motion kinematics

Modelling ECM machining involves determining interelectrode gap thickness changes, the shape evolution of the machined surface, and distribution of physico-chemical conditions occurring within the machining area, such as: static pressure distribution, electrolyte flow velocity, temperature and volume fraction. Physical phenomena occurring in the interelectrode gap are described by partial different equation system resulting from the balance of mass and energy of the flowing electrolyte in the gap [3]. The shape change of the workpiece (WP) is caused by irregularity of anode dissolution velocity. In case of electrochemical machining ECM, and especially with a vibratory TE, the influence of temperature field dependent on hydrodynamic parameters can not be neglected, since the temperature has significant impact on the electrolyte properties, and in consequence on the current density distribution which occur. Correctly determined velocity and temperature distribution, the proper electrolyte conductivity, current density distributions makes it possible to describe the geometry of the workpiece accurately.

2. Mathematical model

The system of equations which describes the two-dimensional electrolyte flow in the interelectrode gap (Fig. 2) results from momentum and mass conservation law [2], [4].

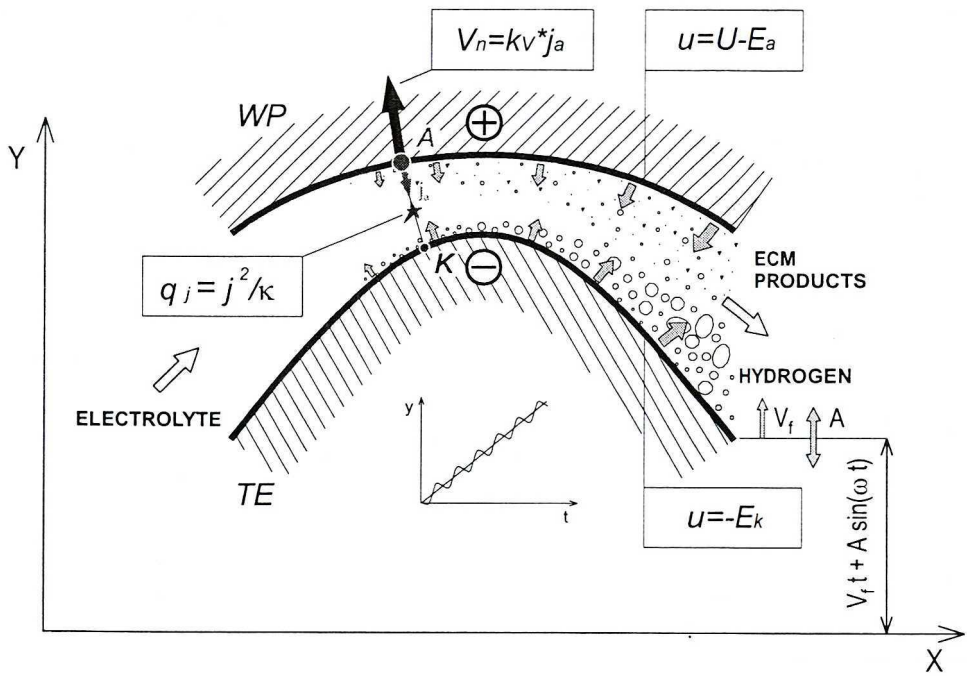

Fig. 2. The interelectrode gap

Equations of motion resulting from the mass conservation law for electrolyte (liquid) and hydrogen (gas) respectively are as following:

$$\frac{\partial}{\partial t}(\rho_e) + \frac{\partial}{\partial x}(\rho_e v_x) + \frac{\partial}{\partial y}(\rho_e v_y) = 0 \tag{1}$$

$$\frac{\partial}{\partial t}(\rho_h) + \frac{\partial}{\partial x}(\rho_h v_x) + \frac{\partial}{\partial y}(\rho_h v_y) = j\eta_H k_H h^{-1} \tag{2}$$

Equations resulting from the principle of conservation of momentum for electrolyte assume the form:

$$\rho_e\left(\frac{\partial v_x}{\partial t} + v_x\frac{\partial v_x}{\partial x} + v_y\frac{\partial v_x}{\partial y}\right) = F_x - \frac{\partial p}{\partial x} + \mu\left(\frac{\partial^2 v_x}{\partial x^2} + \frac{\partial^2 v_x}{\partial y^2}\right) \tag{3}$$

$$\rho_e\left(\frac{\partial v_y}{\partial t} + v_x\frac{\partial v_y}{\partial x} + v_y\frac{\partial v_y}{\partial y}\right) = F_y - \frac{\partial p}{\partial x} + \mu\left(\frac{\partial^2 v_y}{\partial x^2} + \frac{\partial^2 v_y}{\partial y^2}\right) \tag{4}$$

where: v_x, v_y – components of flow velocity,
p – pressure,
F_x, F_y – components of force,
$\rho_e = \rho_{eo}(1 - \beta)$ – electrolyte density,
$\rho_h = \rho_{Ho}\beta$ – hydrogen density,
β – volume fraction,

Equations resulting from conservation of energy law for electrolyte assume the form:

$$\frac{\partial}{\partial t}(\rho_e T_e) + \frac{\partial}{\partial x}(\rho_e v_x T_e) + \frac{\partial}{\partial y}(\rho_e v_y T_e) = \frac{\partial}{\partial y}\left(a\frac{\partial T}{\partial y}\right) + \frac{Q}{c_p} \tag{5}$$

Equations (1÷5) should meet the following boundary conditions:

– for velocity

v_x, $v_y = 0$ for $y = 0$
$v_x = 0$ for $y = h$
$v_y = \dfrac{\partial h}{\partial t}$ for $y = h$
where: $h = h_0 + A\sin(\omega t)$

– for pressure

$p = p_o$ for $x = x_0$

– for temperature

$T = T_0$ for $x \geq x_i$ and $y = 0$ and $y = h$
where:
x_i – the coordinate of IEG inlet,
x_o – the coordinate of IEG outlet,
T_0 – temperature of electrodes.

Electrolyte flow was analyzed in local curvilinear orthogonal coordinate system.

For the solution of equations system resulting from the principle of conservation of momentum and the mass conservation law, the following simplified assumptions were introduced [5]:
– electrolyte flow is stationary, two-dimensional, laminar, and isothermal,
– inertial forces of electrolyte flow are neglected, there is limitation of the so called Reynold's approximation,

- influence of unit mass force is neglected,
- it was assumed that:

$$h(x, t) << L$$

i.e. thickness of the gap is small in comparison with the length of the interelectrode gap.

Accepting the above-mentioned assumptions, the equation system (1÷5) has the following form:

- continuity equation of electrolyte flow:

$$\frac{\partial}{\partial x}(\rho_e v_x) + \frac{\partial}{\partial y}(\rho_e v_y) = 0 \tag{6}$$

- continuity equation of hydrogen flow:

$$\frac{\partial}{\partial x}(\rho_h v_x) + \frac{\partial}{\partial y}(\rho_h v_y) = j\eta_H k_H h^{-1} \tag{7}$$

- equation resulting from principle of conservation of momentum
  - for x direction

$$\frac{\partial^2 v_x}{\partial y^2} = \frac{1}{\mu}\frac{\partial p}{\partial x} \tag{8}$$

  - for y direction

$$\frac{\partial p}{\partial y} = 0 \tag{9}$$

  - conservation of energ-y

$$v_x\frac{\partial T}{\partial x} + v_y\frac{\partial T}{\partial y} = a\frac{\partial^2 T}{\partial y^2} + \frac{Q}{\rho_e c_p} \tag{10}$$

From the equation (9) it results that $p = p(x)$

After integrating the equation (8) and taking into consideration boundary conditions we have:

$$v_x = \frac{1}{2\mu}\frac{dp}{dx}(y^2 - yh) \tag{11}$$

Let us introduce to our considerations the concept of flow rate:

$$Q_V = \int_0^h v_x dx \tag{12}$$

thus, after transformation we obtain:

$$\frac{dp}{dx} = -\frac{12\mu Q_V}{h^3} \tag{13}$$

so that

$$v_x = \frac{6Q_V}{h^3}(y^2 - yh) \tag{14}$$

Substituting equation of electrolyte flow (6) the velocity distribution (14) into continuity, then integrating, we obtain the component v_y in the form:

$$v_y = \frac{-6Q_V}{h^6}(h^2h'y^3 - h'h^3y^2) \tag{15}$$

Integrating equation (13) and respecting border conditions for pressure we obtain:

$$p = p_z - 12\mu Q_V(A(x) - Ao) \tag{16}$$

where $A(x) = \int\frac{dx}{h^3}$, $Ao = A(x_o)$

Equation which describes the volume fraction is obtained on the basis of balance of gas mass flowing across IEG:

$$\frac{\partial(\rho_H v_x)}{\partial x} + \frac{\partial(\rho_h v_y)}{\partial y} = \eta_H k_H j h^{-1} \tag{17}$$

Assuming that the concentration of is changing along the interelectrode gap, i.e. $\beta = \beta(x)$, after integrating equation (17) across the gap we obtain:

$$\frac{\partial}{\partial x}\rho_H \int_0^h v_x dy + \rho_H v_y \Big|_0^h = \eta_H k_H j \tag{18}$$

for the case without vibrations

$$\frac{\partial \rho_H}{\partial x} = \frac{\eta_H k_H j}{Q_V} \tag{19}$$

where

$$\rho_H = \beta\, \rho_{Ho}, \quad \rho_{Ho} = \frac{\mu_H p}{R_H T} \tag{20}$$

μ_H – hydrogen molar mass,
R_H – gas constant,
$h(x)$ – local height of interelectrode gap,
ρ_{Ho} – hydrogen density.

Introducing equation (19) and the function describing current density [1], [3] to equation (18) we obtain:

$$j = \frac{\kappa_0 \Phi_{TG}^{-1}(U - E)}{h} \tag{21}$$

and:

$$\frac{\partial \beta}{\partial x} = \frac{\eta_H k_H R_H}{\mu_H} \frac{\kappa_0 \Phi_{TG}^{-1}(U - E)}{Q_V h} \frac{T}{p} \tag{22}$$

Integrating the equation (22) and taking into consideration that $\beta = 0$, when $x = x_0$ we obtain a formula, which describes distribution of volume fraction:

$$\beta = \frac{\eta_H k_H R_H}{\mu_H} \frac{\kappa_0 \Phi_{TG}^{-1}(U - E)}{Q_V h} \frac{T}{p} x \tag{23}$$

The equation allowing us to determine temperature distribution in the gap (10) was solved numerically with the method of finite differences using velocity distributions v_x and v_y described by formulae (14) and (15).

The obtained solutions let us describe velocities of electrochemical dissolution of the machined surface. This velocity is described by equation [1]:

$$\frac{\partial Y_A}{\partial t} = k_v \kappa_0 \Phi_{TG}^{-1} \frac{U - E}{d_{\min}} \sqrt{1 + \left(\frac{\partial Y}{\partial x}\right)^2} \tag{24}$$

$$\Phi_{TG} = \frac{1}{h}\left[\int_0^h \frac{dy}{(1 + \alpha_T (T - T_0)(1 - \beta)^{3/2}}\right] \tag{25}$$

where:

k_v – coefficient of electrochemical machining,
α_T – temperature coefficient of electrical conductivity,
κ_o – electrolyte conductivity at T_i and $\beta = 0$.

3. Numerical model of the process ECM

Determination of the machined surfaces shape in time is described by equation (24) defining the real shape change of the machined surface.

Equation (24) was solved with the use of successive approximation method for all the used numerical schemes (Fig. 3) using simultaneously a method of time steps [6], [7].

Time coordinate t has been presented by a set of points:

$$t_k = t_0 + k\,\Delta t$$

where:

$$k = 0, 1, 2, \ldots K$$

Time step has been matched to every vibration frequency so that one vibration period can be described by at least 12 points. After discretization of the time, the solution scheme was divided into stages for every time step:

- discretization WP (workpiece) and TE (tool-electrode) in a global rectangular coordinate system:

$$x_i = x_0 + i\,\Delta x$$

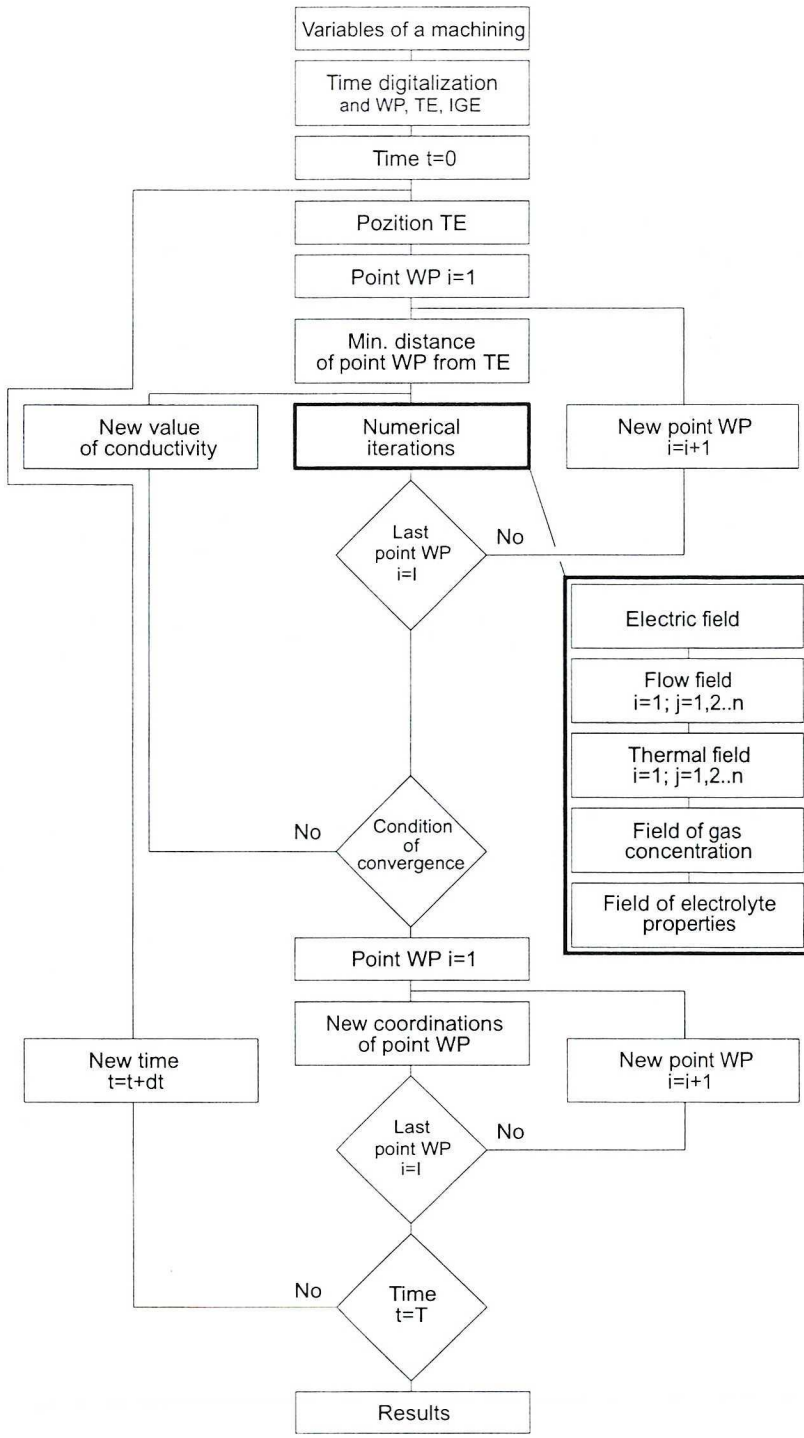

Fig. 3. Scheme of chart at simulation ECM

where

$i = 0, 1, 2, ... I,$

$\Delta x = \frac{L}{i},$

L – length WP in the direction to axis x,

- computing for each time step the minimal distance of the discussed A point on WP from TE through comparison of distances to all points of digitized TE: $h_n = min\,(d)$,
- discretization of IEG (Fig. 4) along the earlier determined distance d_{min}.

In locally orthogonal coordinate system in the point A we receive:

$$y_i' = j\,\Delta y'$$

where j = 0, 1, 2, ... J $\quad \Delta y' = \frac{d_{min}}{j}$

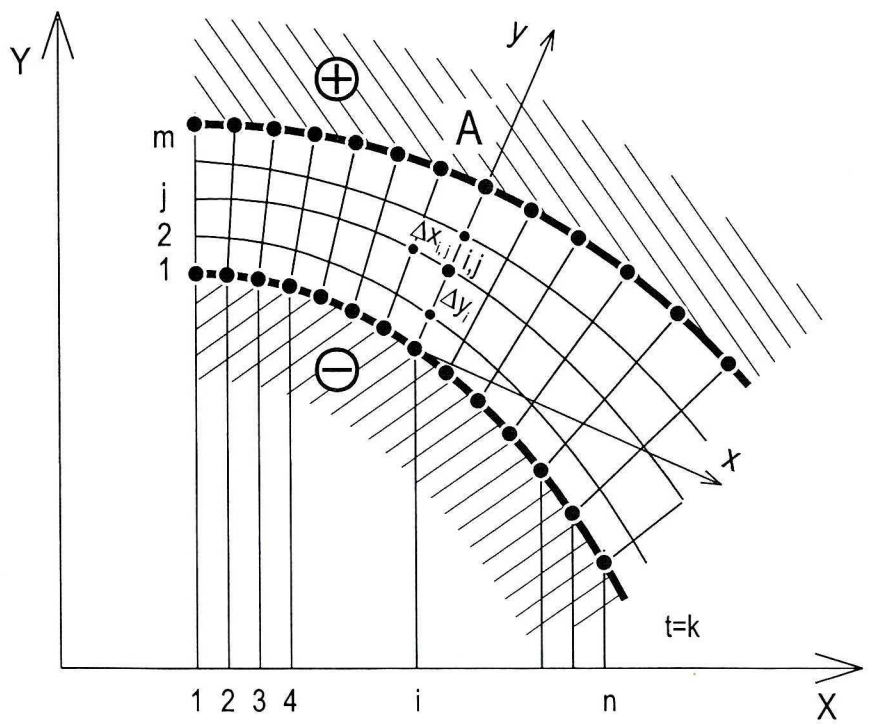

Fig. 4. Discretization of interelectrode gap

- Calculation of current density field j_A in the discussed point A (in the first time step for the accepted value k), with the assumed polarization of the cathode described by Tafel's equation [1],

- Calculation of the flow field area in a locally orthogonal system of coordinates (in the first time step for accepted values κ, β, p, v) calculation of temperature field in a locally orthogonal system of coordinates,
- Calculation of conductivity field $\kappa(x, y)$ of the electrolyte for updated values of temperature,
- Calculation of the volume fraction $\beta(x)$ from the mass balance equation,
- Calculation of the medium properties parameters viscosity $\mu(x, y)$ and density $p(x, y)$,
- Calculation of new coordinates of points WP in the global rectangular coordinate system using Euler'a method for solving partial equations,
- Going on to the next time step-time in the discussed scheme plays the role of a parameter, a series of calculations is created which are performed with "frozen" gap thickness distribution for each time step.

A computer program for simulation of electrochemical manufacturing process has been created. In figures 5÷7 a flowchart of numerical algorithm is presented.

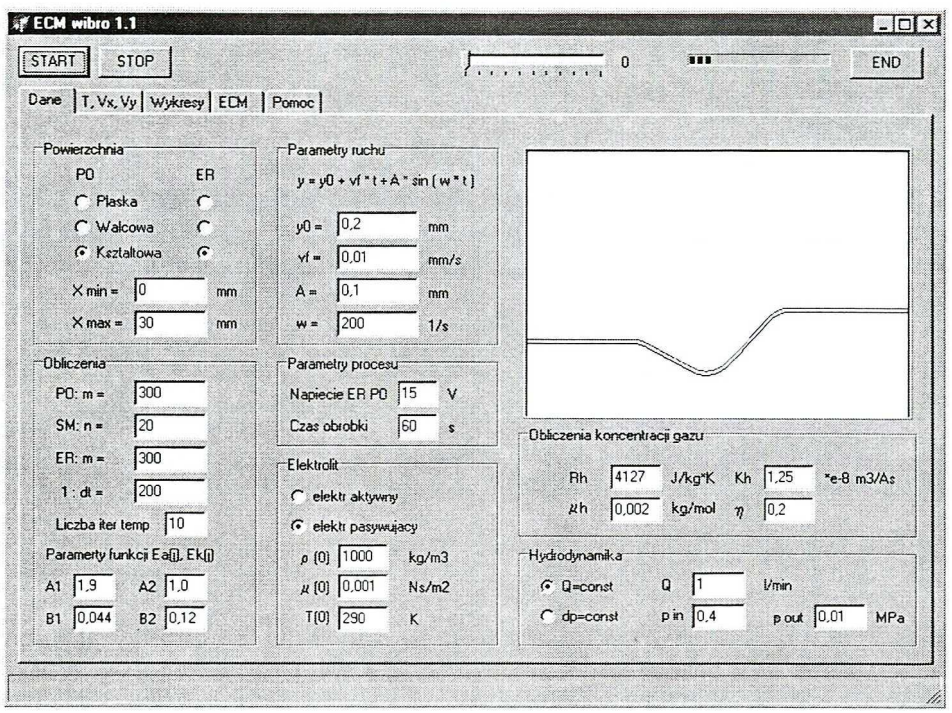

Fig. 5. Computer application figure "Data"

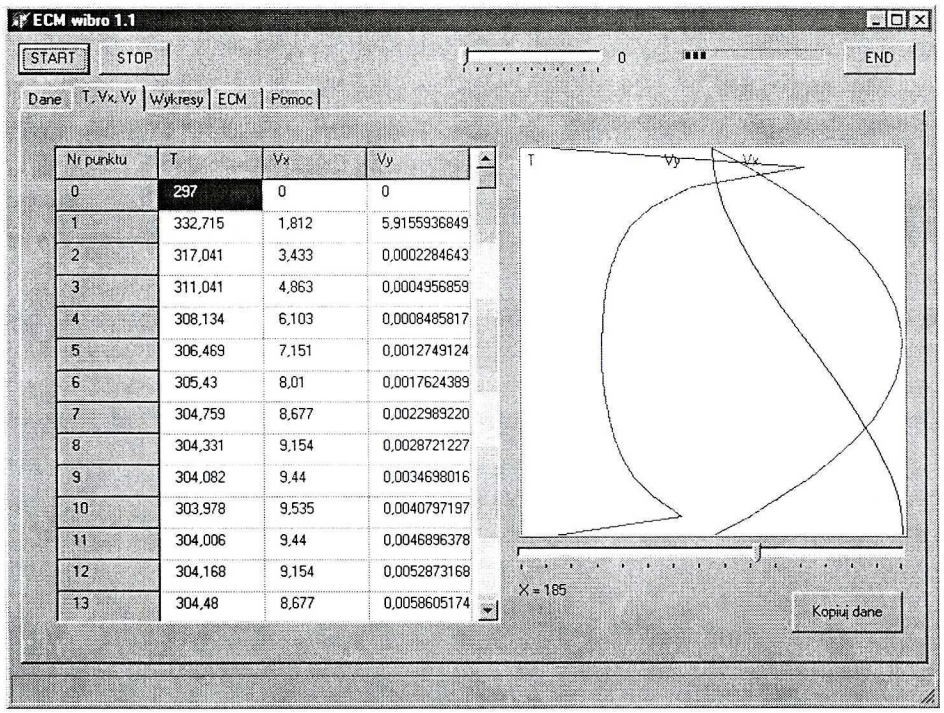

Fig. 6. Computer application figure "Results"

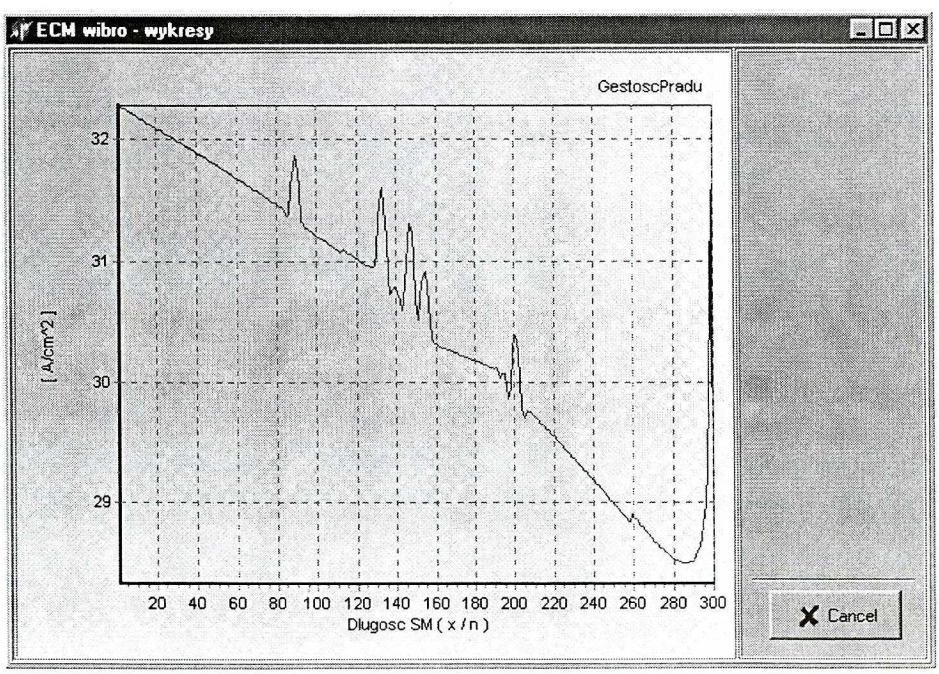

Fig. 7. Computer application figure "Graph" – current density

4. Calculation results

The calculations were performed for electrodes with geometrical features shown in figure 8. Calculations were performed until obtaining the quasi-stationary state. More important parameters of machining are shown in Table 1.

Table 1.

Important parameters of machining

Initial gap	0.2 mm
Velocity of feed motion TE	0.0125 mm/s
Interelectrode voltage	15 V
Vibration amplitude	0.13 mm
Vibration frequency	17,5 Hz

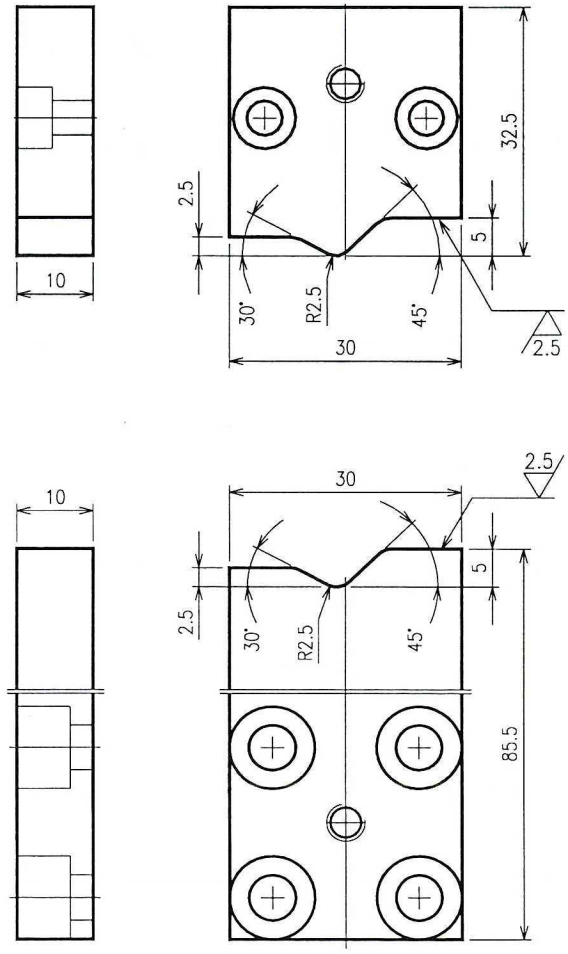

Fig. 8. Geometrical features of electrodes

The calculations were performed for the case without vibrations and with a vibrating electrode. In the first, the case calculations were being performed until the steady state was reached, in the second case until a quasi – stationary state was reached, that is when the interelectrode gap thickness changes and physical conditions between electrodes in time became periodical.

The diagrams in Figs. 9÷13 depict distribution of thickness h of interelectrode gap, pressure p, mean velocity of electrolyte flow v_{mean}, current density j, and of gas concentration β along interelectrode gap for the case without vibrations.

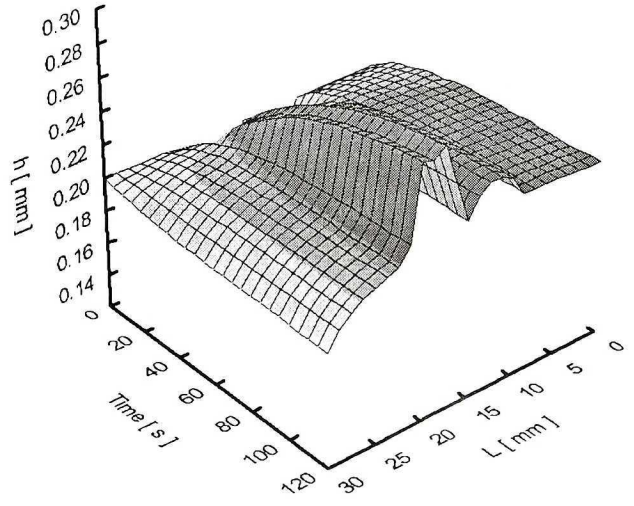

Fig. 9. Thickness h IGE distribution along its length

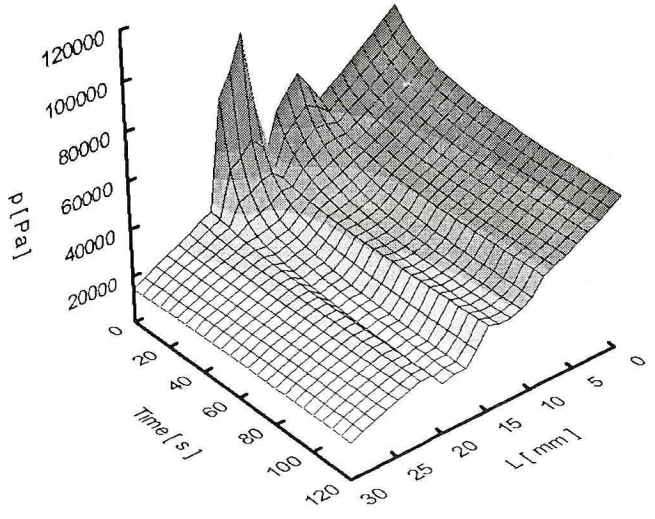

Fig. 10. Pressure p distribution along IGE

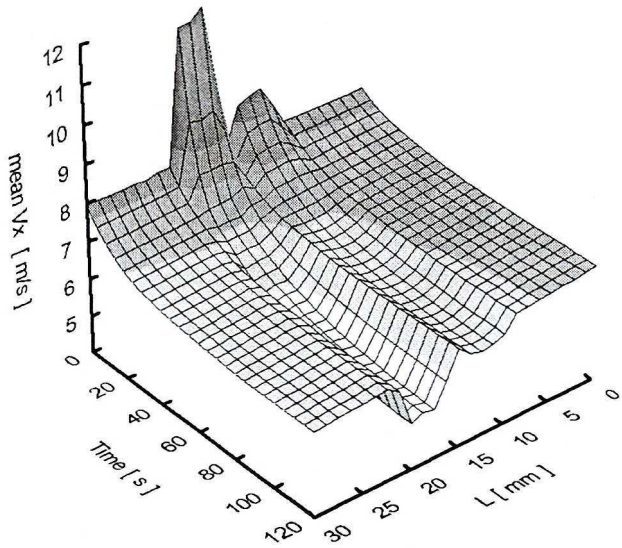

Fig. 11. Velocity $v_{x\ mean}$ distribution along IGE

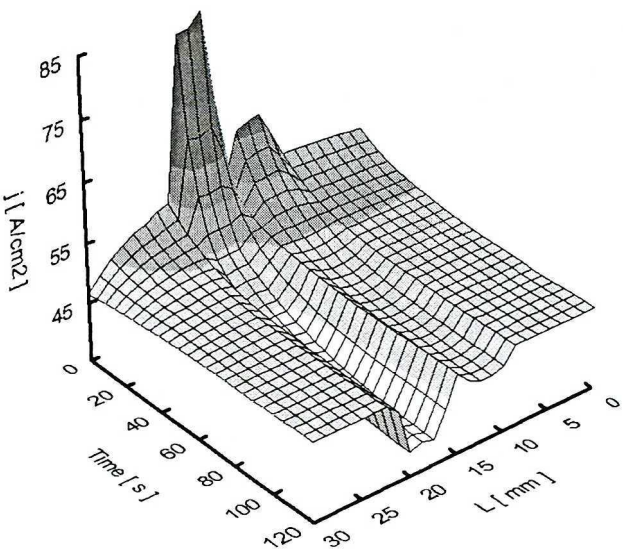

Fig. 12. Current density distribution along IGE

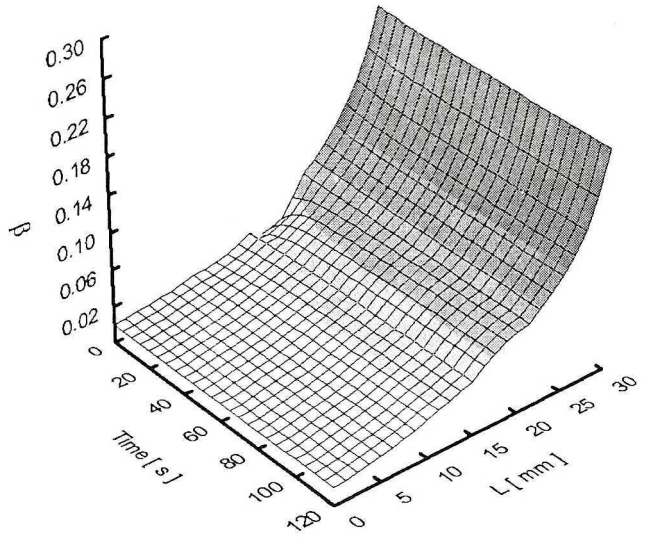

Fig. 13. Volume fraction β distribution along IEG

On the basis of the obtained calculation results illustrated by charts, the following conclusions can be formulated:

- Current density distribution (Fig. 12) shows that the ECM machining process is subject to self regulation. It means stabilization of other physical values at a constant level in such a way that the current density distribution stabilizes at the constant level,
- Separation of gasous phase in the interelectrode gap affects the medium properties such as conductivity, density and viscosity. It changes hydrodynamic conditions which occur in the gap which is caused by pressure distributions (Fig. 10), and electrolyte flow velocity (Fig. 11),
- Separation of gasous phase (hydrogen) in the interelectrode gap (Fig. 13) makes the electrochemical dissolution process more difficult. The volume fraction increase, especially in the final part of the gap, causes machining efficiency decrease.

The diagrams in Figs. 14÷18 illustrate distribution of thickness h of the IEG, pressure p, mean velocity of the electrolyte flow v_{mean}, current density j, and of gas concentration β along the IEG for the case with a vibrating electrode for one vibration period. Additionally, fig. 19 presents calculation results of the electrolyte temperature in the transverse cross section distant 20 mm from the interelectrode gap beginning for one vibration period.

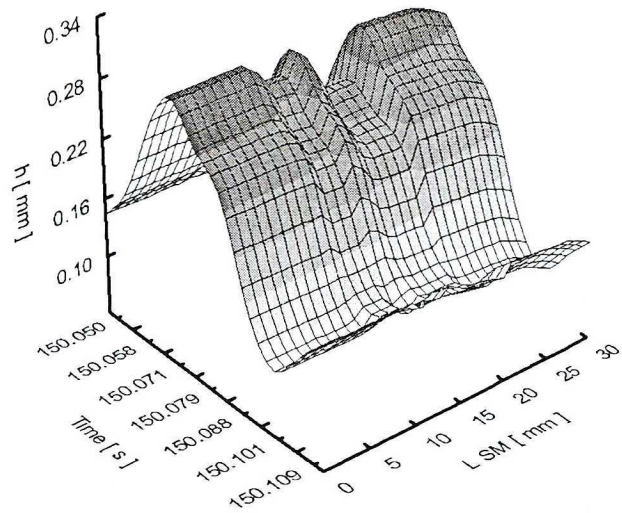

Fig. 14. Thickness h IGE distribution along its length

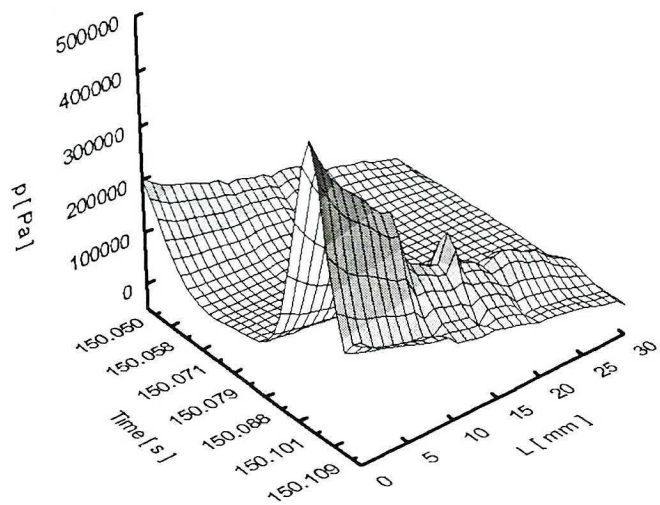

Fig. 15. Pressure p distribution along IGE

Local gap thicknesses IEG (Fig. 14) change. It is caused by electrochemical dissolution velocity changes, the tool electrode angle of inclination profile in relation to the electrochemical machining direction, and physical conditions variability along the flow. Using passivating electrolyte results in deformation of sinusoidal course of thickness changes along the time axis.

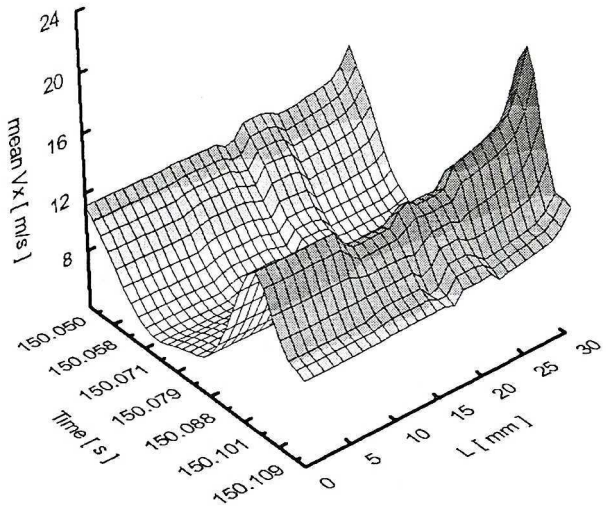

Fig. 16. Velocity v_x distribution along IGE

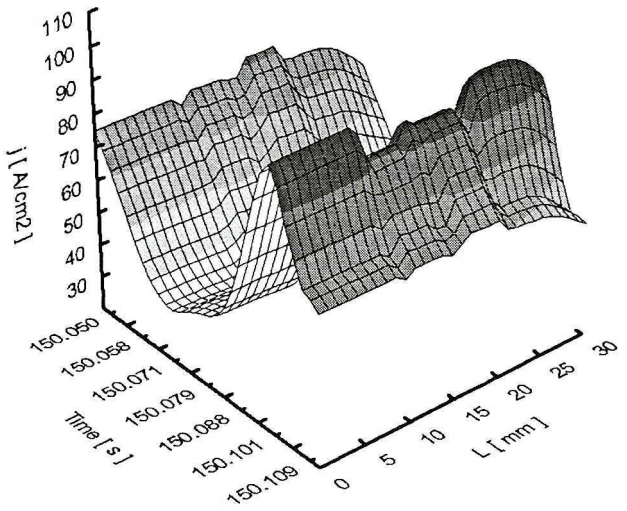

Fig. 17. Current density distribution along IGE

Maximal values $\beta = 0.27$ (Fig. 18) are significantly lower than the boundary values and they occur in the time in which there are higher IEG thicknesses.

In the case of minimum IEG, there occur high electrolyte flow pressures and velocities and despite big current densities falling on this moment (Fig. 17) the values β are not maximum. It is very advantageous from the point of view of the TE shape representation accuracy.

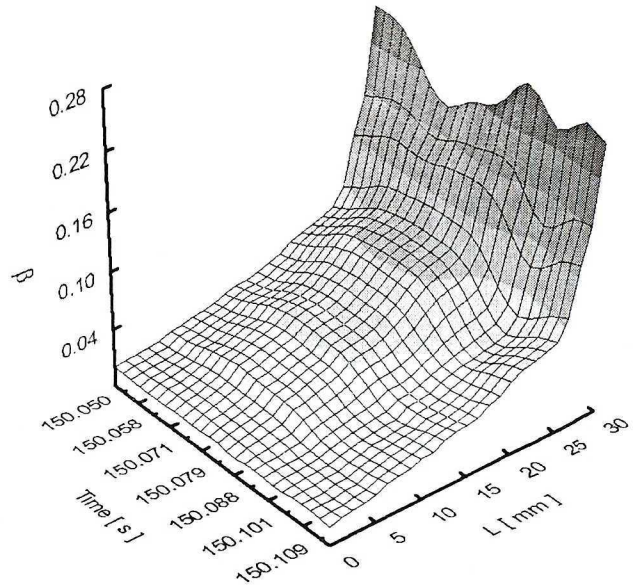

Fig. 18. Volume fraction β distribution along IEG

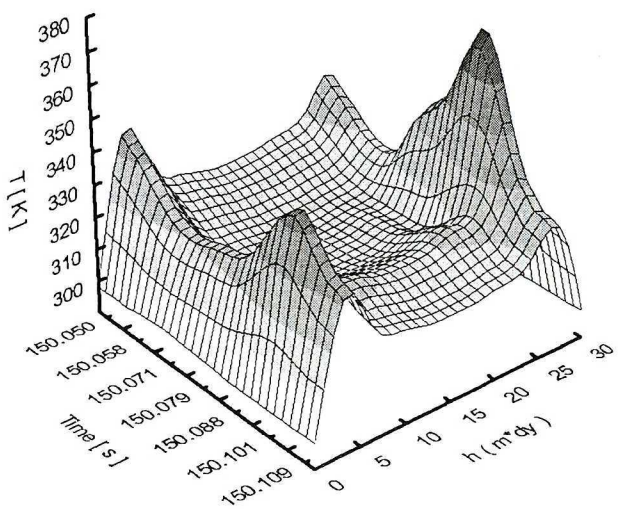

Fig. 19. Temperature T distribution along IGE thickness

The characteristic feature of the presented temperature distribution of the electrolyte (Fig. 19) is the occurrence of extreme values near the electrodes which change depending on location of the vibrating tool-electrode. Maximal temperature values occur at the moment of time which at electrodes approach one another at the minimal distance. The influence on the character of

electrolyte temperature changes near the vibrating TE wall was exerted by velocity v_y resulting from vibrations. This is one of the reasons causing temperature distribution asymmetry. Determining the temperature distributions along the gap thickness, which significantly vary from the mean temperature for a given cross-section, has a great significance for more accurate machining parameter choice.

5. Experimental verification of mathematical model

The tests verifying mathematical model of ECM process with a vibrating electrode were carried out comparing the WP profile, which was obtained in result of computer simulation, with the process whose profile was obtained in result of machining (Fig. 20).

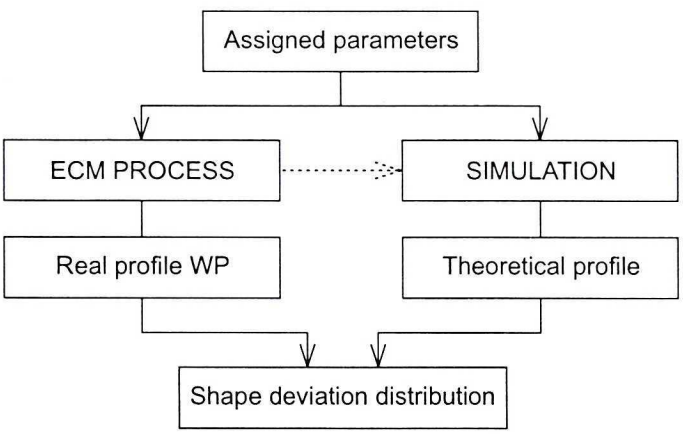

Fig. 20. Algorithm of tests verifying mathematical model of ECM process

The obtained profiles were approached to each other along the axis z as long as the standard deviation value S obtained the minimal value. It enabled us to determine the shape deviation distribution measured along the WP area in relation to the shape achieved from simulation.

In figure 21 the scheme of the experimental setup is presented. The fundamental element of the station is the machining cell, where the WP and the TE are placed. The cell is made of a transparent material, which allows for observation of the electrodes and the electrolyte flow. The electrolyte flows through the inter-electrode gap in such a way that it achieves the conditions of the plane parallel flow as closely as possible. Vibrations are caused by an electrodynamic inductor WED-O4. The end of the inductor is connected with the TE through a slide placed on a guide. On the same guide there is another slide placed together with the WP in the machining cell.

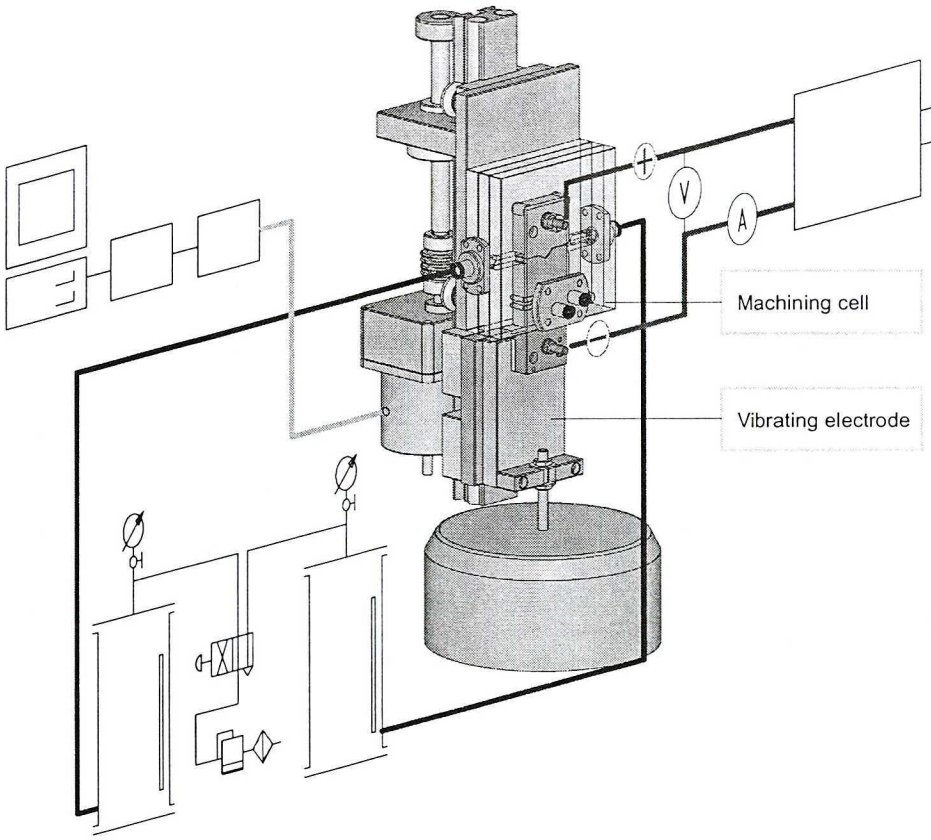

Fig. 21. The experimental setup scheme

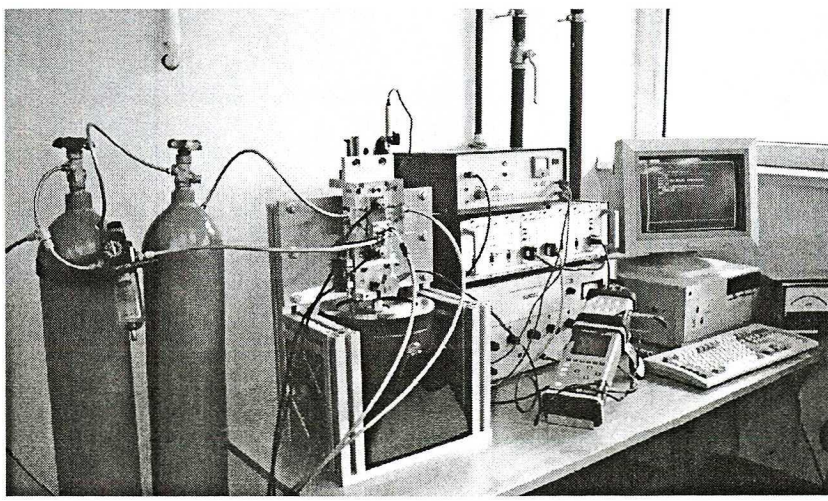

Fig. 22. The test station

The machining cell, together with the WP, moves with the translate motion at constant velocity. The cell is driven by a stepper motor. The graphs in figure 21 show the power supply and electrolyte supply of the machining cell are presented.

Figure 22 presents the test station with the controlling and measuring equipment used in the tests.

In the charts (Table 2), the shape deviation distributions (thick line, down) and the shape of the working electrode (thin line, up) are presented as well as precision indexes accepted for evaluation.

It results from the shape deviation distribution that maximal deviations occur in the sectors which are curvature radii. It is caused by electrical field potential linearization error along the ME gap thickness.

Table 2.

For the case without vibrations	
S	0.0124 mm
δ_{mean}	0.0251 mm

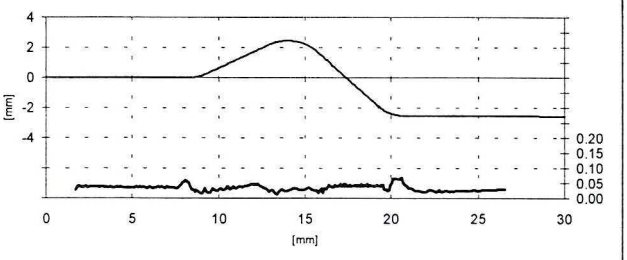

For the case with a vibrating electrode	
S	0.0118 mm
δ_{mean}	0.0197 mm

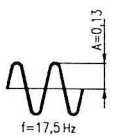

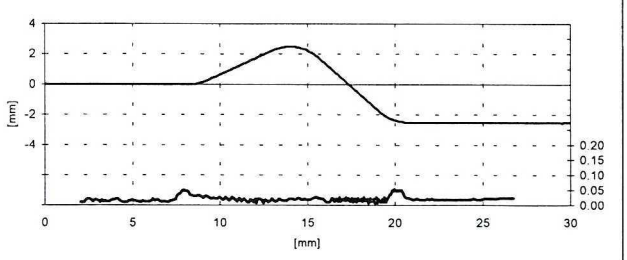

For the case with a vibrating electrode	
S	0.0152 mm
δ_{mean}	0.0382 mm

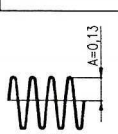

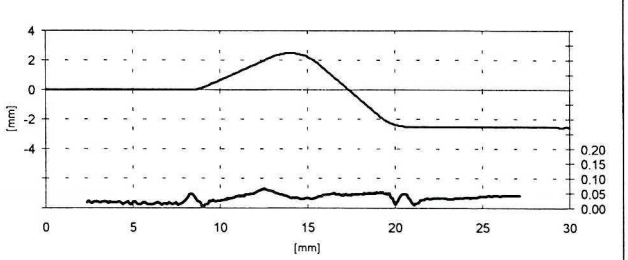

The best calculation results were obtained for smaller vibration frequencies. Along with the frequency and vibration amplitude increase, the accuracy of the examined model deteriorates. Dynamic phenomena in the flow become more significant, and in consequence the flow becomes not stabilized.

Manuscript received by Editorial Board, June 30, 2004;
final version, September 15, 2004.

REFERENCES

[1] Dabrowski L.: Podstawy komputerowej symulacji kształtowania elektrochemicznego (Basic of the computer simulation of electrochemical shaping). Prace Naukowe, Mechanika z. 154, Wydawnictwo Politechniki Warszawskiej, Warszawa, 1992 (in Polish).

[2] Kozak J.: Kształtowanie powierzchni obróbką elektrochemiczną bezstykową (Electrochemical shaping (ECM)). Prace Naukowe PW, Mechanika nr 41, Wydawnictwo Politechniki Warszawskiej, Warszawa, 1976 (in Polish).

[3] Kozak J.: Mathematical models for computer simulation of electrochemical machining processes. Journal of Materials Processing Technology 76. May 1997.

[4] Volgin V. M., Lyubimov V. V.: Mathematical Modeling of three-dimensional electrochemical forming of complicated surfaces. Proceedings International Conference APE'98. Warszawa 1998.

[5] Paczkowski T., Sawicki J.: Wpływ koncentracji wodoru w elektrolicie na ewolucję kształtu przedmiotu obrabianego ECM (Effects of hydrogen void fraction on process shaping in ECM). Materiały konferencyjne EM'03. Bydgoszcz – Rydzyna. 2003 (in Polish).

[6] Kozak J.: Komputerowe wspomagania technologii drążenia elektrochemicznego (Computer aided manufacturing system for electrochemical sinking). SNOE nr 5, Warszawa 1999 (in Polish).

[7] Filatov E.: The Numerical Simulation of the Unsteady ECM Process. Proceedings International Conference APE'98. Warszawa, 1998.

Komputerowa symulacja zjawisk zachodzących w 2D szczelinie międzyelektrodowej podczas elektrochemicznej obróbki z drgającą elektrodą

Streszczenie

Autorzy przedstawiają dwuwymiarowy model matematyczny i numeryczny przepływu elektrolitu w szczelinie międzyelektrodowej. Przedstawiony program komputerowy umożliwia wizualizację zjawisk zachodzących w szczelinie międzyelektrodowej w czasie obróbki z drgającą elektrodą. Umożliwia on śledzenie rozkładu ciśnień, prędkości, zmian przepływu, rozkładu i zmian temperatur i co najważniejsze – śledzenie zmian kształtu przedmiotu obrabianego w funkcji zmian parametrów procesu obróbki. Wyniki modelowania i symulacji komputerowej zweryfikowano doświadczalnie.